SFB/CPP-08-75
TTP/08-25

Matching coefficients for α_s and m_b to $\mathcal{O}(\alpha_s^2)$ in the MSSM

A. Bauer, L. Mihaila, J. Salomon

Institut für Theoretische Teilchenphysik, Universität Karlsruhe (TH),

Karlsruhe Institute of Technology (KIT)

76128 Karlsruhe, Germany

Abstract

We compute the exact two-loop matching coefficients for the strong coupling constant α_s and the bottom-quark mass m_b within the Minimal Supersymmetric Standard Model (MSSM), taking into account $\mathcal{O}(\alpha_s^2)$ contributions from Supersymmetric Quantum Chromodynamics (SQCD). We find that the explicit mass pattern of the supersymmetric particles has a significant impact on the predictions of α_s and m_b at high energies. Further on, the three-loop corrections exceed the uncertainty due to the current experimental accuracy. In case of the the running bottom-quark mass, they can reach in the large $\tan\beta$ regime up to 30% from the tree-level value.

PACS numbers: 11.30.Pb, 12.38.-t, 12.38.Bx, 12.10.Kt

1 Introduction

Supersymmetry (SUSY) is currently believed to play an important role in physics beyond the Standard Model (SM). A compelling argument in favour of SUSY is the particle content of the MSSM, that leads in a natural way to the unification of the three gauge couplings at a high energy scale $\mu \simeq 10^{16}$ GeV, in agreement with predictions of Grand Unification Theories (GUT) [1–3].
Apart from the gauge coupling unification, in GUT models based on simple groups such as $SU(5)$ [4] or $SO(10)$ [5], also the top (y_t), bottom (y_b), and tau (y_τ) Yukawa couplings unify at the GUT scale. However, the condition of Yukawa coupling unification can be fulfilled within the MSSM only for values of $\tan\beta$, the ratio of Higgs field vacuum expectation values, of about 50 [6, 7]. A main feature of SUSY models with large $\tan\beta$ is that the supersymmetric radiative corrections to fermion masses and couplings can be as large as the leading order (LO) contributions [8]. This renders the knowledge of the higher order (HO) corrections in perturbation theory mandatory. On the other hand, the unification condition becomes very sensitive to the low energy parameters [9]. This property can be exploited to greatly constrain the allowed MSSM parameter space.

With the advent of the CERN Large Hadron Collider (LHC), we will be able to probe the realization of SUSY in nature to energy scales of $\mathcal{O}(1)$ TeV. In particular, precision measurements and computations will allow to test the low-energy supersymmetric relations between the particle masses and couplings. It is often argued (for reviews see e.g. Refs. [10, 11]) that, from the precise knowledge of the low-energy supersymmetric parameters one can shed light on the origin and mechanism of supersymmetry breaking and even on physics at much higher energies, like the GUT scale. The extrapolation of the supersymmetric parameters measured at the TeV energy scale to the GUT-scale raises inevitably the question of uncertainties involved. Currently, there are four publicly available spectrum generating codes [12–15] based on two-loop order MSSM renormalization group equations (RGEs) [16–19] subjected to two types of boundary conditions. One set of constraints accounts for the weak-scale matching between the MSSM and SM parameters to one-loop order [20]. The second one allows for the SUSY breaking at the high scale according to specific models like minimal supergravity, gauge mediation and anomaly mediation. The approximations within the codes differ by high-order corrections and by the treatment of the low-energy threshold corrections. The typical spread of the results is within few percents, which does not always meet the experimental accuracy [21]. Along the same line, recent analyses [22, 23] have proven that the three-loop order effects on the running of the strong coupling constant α_s and the bottom quark mass m_b may exceed those induced by the current experimental accuracy [24, 25].
Very recently, Ref. [26] computed the two-loop SQCD and top-induced Supersymmetric Electroweak (SEW) corrections to the effective bottom Yukawa couplings. The knowledge of the two-loop corrections allows predictions for the branching ratios of the MSSM Higgs bosons with per-cent level accuracy.

The aim of this paper is to compute the two-loop decoupling relations for the strong coupling constant and the bottom quark mass, taking into account the exact dependence on the particle masses. This will extend the study of Ref. [22] allowing phenomenological analyses based on quasi-realistic mass spectra for SUSY particles, with three-loop order accuracy. However, we will consider in this paper only the $\mathcal{O}(\alpha_s^2)$ corrections from SQCD and postpone the study of the SEW contributions $\mathcal{O}(\alpha_s y_t^2, \alpha_s y_b^2, y_t^4, y_t^2 y_b^2, y_b^4)$ to further investigations. Whereas the SEW corrections to the decoupling coefficient of α_s are expected to be negligible, their numerical impact on the running bottom quark mass can become as important as those from SQCD. At the one-loop order [20], the main contributions to the bottom-quark mass decoupling coefficient arise from diagrams containing gluino- and Higgsino-exchange. In the most regions of the MSSM parameter space the gluino contribution is the dominant one and can be as large as the tree-level bottom quark mass. However, there are domains in the parameter space where the corrections due to gluino- and Higgsino-exchange can become of the same order and have opposite sign. These regions contain the special points for which the Yukawa coupling unification occurs [9, 27]. For the MSSM parameters for which the radiative corrections to the bottom quark mass are comparable with the LO ones, Ref. [28] proposed a method to resum them to all orders in perturbation theory. A numerical comparison with the results of Ref. [28] can be found in Section 5.

The paper is organized as follows: in Section 2 and Section 3 we discuss the theoretical framework and the renormalization scheme we use. In Section 4 we present the analytical one- and two-loop results. The latter ones are displayed in analytical form for three simplifying mass hierarchies among the SUSY particles. The numerical effects are studied in Section 5.

2 Framework

As already stated above, the underlying motivation for the running analysis is to relate physical parameters measured at the electroweak scale with the Lagrange parameters at the GUT scale. The running parameters are most conveniently defined in mass-independent renormalization schemes such as $\overline{\rm MS}$ [29] for the SM parameters and $\overline{\rm DR}$ [30] for the MSSM parameters. It is well known that in such "unphysical" renormalization schemes the Appelquist-Carazzone decoupling theorem [31] does not hold in its naive form. Quantum corrections to low-energy processes contain logarithmically enhanced contributions from heavy particles with masses much greater than the energy-scale of the process under consideration. An elegant approach to get rid of this unwanted behaviour in the $\overline{\rm MS}$ or $\overline{\rm DR}$ scheme is to formulate an effective theory (ET) [32, 33] integrating out all heavy particles. The coupling constants defined within the ET must be modified in order to account for the effects of the heavy fields. They are related with the parameters of the full theory by the so-called matching or decoupling relations.

For moderate mass splittings between SUSY particles, *i.e.* there are no large logarithms in the theory that have to be resummed by means of RGEs, the decoupling of heavy particles might be performed in one step [34]. The energy-scale at which the decoupling is performed is not fixed by the theory. It is usually chosen to be $\mu \simeq \tilde{M}$, where $\tilde{M}$ is a typical heavy particle mass. The MSSM parameters at energies $E \simeq \tilde{M}$ can be determined from the knowledge of the corresponding SM parameters and the associated decoupling relations.

The decoupling coefficients for the strong coupling constant and for the light quark masses are known in QCD with four- [35, 36] and three-loop [32] accuracy, respectively. Due to the presence of many mass scales, their computation within SQCD and SEW is quite involved. At one-loop order, they are known exactly [20, 37]. At two-loop order, the decoupling coefficient for the strong coupling is known only for specific mass hierarchies [22]. Recently, the two-loop SQCD corrections for the decoupling coefficient of the bottom-quark mass was computed [37]. The focus of this paper is the analytical calculation of the decoupling relations for these parameters within SQCD through two-loops.

We consider SQCD with n_f active quark and $n_s = n_f$ active squark flavours and $n_{\tilde{g}} = 1$ gluinos. Furthermore, we assume that $n_l = 5$ quarks are light (among which the bottom quark) and that the top quark and all squarks and the gluino are heavy. Integrating out the heavy fields from the full SQCD Lagrangian, we obtain the Lagrange density corresponding to the effective QCD with n_l light quarks plus non-renormalizable interactions. The latter are suppressed by negative powers of the heavy masses and will be neglected here. The effective Lagrangian can be written as follows:

$$\mathcal{L}'(g_s^0, m_q^0, \xi^0; \psi_q^0, G_\mu^{0,a}, c^{0,a}; \zeta_i^0) = \mathcal{L}^{SQCD}(g_s^{0\prime}, m_q^{0\prime}, \xi^{0\prime}; \psi_q^{0\prime}, G_\mu^{0\prime,a}, c^{0\prime,a}) \,, \tag{1}$$

where ψ_q, G_μ^a, c^a denote the light-quark, the gluon and the ghost fields, respectively, m_q stands for the light quark masses, ξ is the gauge parameter and $g_s = \sqrt{4\pi\alpha_s}$ is the strong coupling. The index 0 marks bare quantities. $\mathcal{L}^{SQCD}$ is the usual SQCD Lagrangian from which all heavy fields have been discarded. As a result the fields, masses and couplings associated with light particles have to be rescaled. They are labeled by a prime in Eq. (1) and are related with the original parameters through decoupling relations:

$$\begin{aligned} g_s^{0\prime} &= \zeta_g^0 g_s^0 \,, & m_q^{0\prime} &= \zeta_m^0 m_q^0 \,, & \xi^{0\prime} - 1 &= \zeta_3^0(\xi^0 - 1) \,, \\ \psi_q^{0\prime} &= \sqrt{\zeta_2^0}\psi_q^0 \,, & G_\mu^{0\prime,a} &= \sqrt{\zeta_3^0} G_\mu^{0,a} \,, & c^{0\prime,a} &= \sqrt{\tilde{\zeta}_3^0} c^{0,a} \,. \end{aligned} \tag{2}$$

Refs. [32] showed that the bare decoupling constants ζ_m^0, ζ_2^0, $\zeta_3^0, \tilde{\zeta}_3^0$ can be derived from the quark, the gluon and the ghost propagators, all evaluated at vanishing external momenta. As a result, for calculations performed within the framework of Dimensional Regularization/Reduction (DREG/DRED) only the diagrams containing at least one heavy particle inside the loops do not vanish. In Fig. 1 are shown sample Feynman diagrams contributing to the decoupling coefficients for the strong coupling (a) and the bottom-quark mass (b).

For the computation of ζ_g one has to use the well-known Ward identities. A convenient choice is the relation:

$$\zeta_g^0 = \frac{\tilde{\zeta}_1^0}{\tilde{\zeta}_3^0\sqrt{\zeta_3^0}} \,, \tag{3}$$

where $\tilde{\zeta}_1^0$ denotes the decoupling constant for the ghost-gluon vertex.
The finite decoupling coefficients are obtained upon the renormalization of the bare parameters. They are given by

$$\zeta_g = \frac{Z_g}{Z_g'}\zeta_g^0 \,, \quad \zeta_m = \frac{Z_m}{Z_m'}\zeta_m^0 \,, \tag{4}$$

where Z_g' and Z_m' correspond to the renormalization constants in the effective theory. Since we are interested in the two-loop results for ζ_i, $i = g, m$, the corresponding renormalization constants for SQCD and QCD have to be implemented with the same accuracy. Analytical results for them can be found in Refs. [18, 33, 38].

As mentioned above, the decoupling coefficients can be related with vacuum integrals. The latter can be recursively reduced to a master-integral [39] using the method of integration by parts [40]. Given the large number of diagrams and occurrence of many different mass scales, we computed them with the help of an automated setup. The

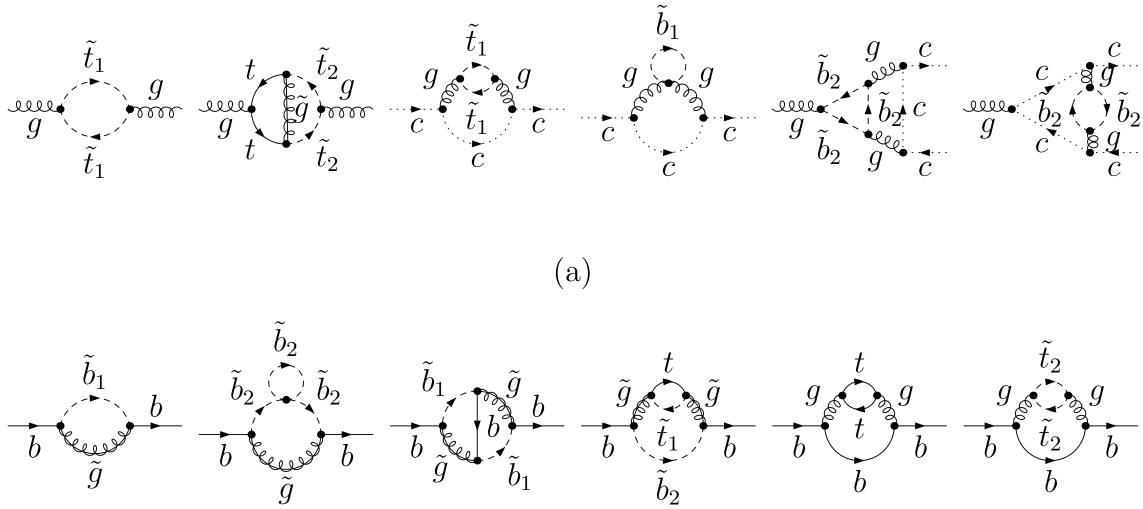

(a)

(b)

Figure 1: Sample diagrams contributing to ζ_3, $\tilde{\zeta}_3$, $\tilde{\zeta}_1$ and ζ_m with gluons (g), ghosts (c), bottom/top quarks (b/t), bottom/top squarks ($\tilde{b}/\tilde{t}$) and gluinos ($\tilde{g}$).

Feynman diagrams were generated with `QGRAF` [41] and further processed with `q2e` [42]. The reduction of various vacuum integrals to the master integral was performed by a self written `FORM` [43] routine. The reduction of topologies with two different massive and one massless lines requires a careful treatment. The related master integral can be easily derived from its general expression valid for massive lines, given in Ref. [39].

3 Regularization and renormalization scheme

In our setup, we used the squark mass eigenstates and their mixing angles as input parameters. For convenience, we give below the relations between them and the parameters of the MSSM Lagrangian.
The squark mass eigenstates $\tilde{q}_{1,2}$ and their mass eigenvalues $m_{\tilde{q}_{1,2}}$ are obtained by diagonalizing the mass matrix

$$\mathcal{M}_{\tilde{q}} = \begin{pmatrix} M_L^2 & m_q X_q \\ m_q X_q & M_R^2 \end{pmatrix} , \tag{5}$$

where we used the notation

$$\begin{aligned} X_q &= A_q - \mu_{\rm SUSY} \left\{ \begin{array}{ll} \tan\beta\,, & \text{for down-type quarks} \\ \cot\beta\,, & \text{for up-type quarks} \end{array} \right. , \\ M_L^2 &= M_{\tilde{Q}}^2 + m_q^2 + M_Z^2 (I_3^q - Q_q s_W^2) \cos 2\beta\,, \\ M_R^2 &= M_{\tilde{D},\tilde{U}}^2 + m_q^2 + M_Z^2 Q_q s_W^2 \cos 2\beta\,. \end{aligned} \tag{6}$$

Here m_q, I_3^q and Q_q are the mass, isospin and electric charge of the quark q, respectively, and $s_W = \sin\theta_W$. The parameters $M_{\tilde{Q}}$ and $M_{\tilde{D},\tilde{U}}$ are the soft supersymmetry breaking masses, A_q is a trilinear coupling and $\mu_{\rm SUSY}$ is the Higgs-Higgsino bilinear coupling.

The squark mass eigenvalues are defined through the unitary transformation

$$\begin{pmatrix} m^2_{\tilde{q}_1} & 0 \\ 0 & m^2_{\tilde{q}_2} \end{pmatrix} = \mathcal{R}_{\tilde{q}} \mathcal{M}_{\tilde{q}} \mathcal{R}^\dagger_{\tilde{q}}\,, \quad \text{with} \quad \mathcal{R}_{\tilde{q}} = \begin{pmatrix} \cos\theta_q & \sin\theta_q \\ -\sin\theta_q & \cos\theta_q \end{pmatrix}\,, \tag{7}$$

and the squark mixing angle through

$$\sin 2\theta_q = \frac{2 m_q X_q}{m^2_{\tilde{q}_1} - m^2_{\tilde{q}_2}}\,. \tag{8}$$

Since we consider the two-loop $\mathcal{O}(\alpha_s^2)$ corrections, only the one-loop $\mathcal{O}(\alpha_s)$ counterterms for the input parameters are required. We have chosen the $\overline{\rm DR}$ scheme to renormalize the strong coupling constant, and the on-shell scheme for the masses of the heavy particles, *i.e.* the gluino, squarks and top quark. The corresponding one-loop renormalization constants are known analytically (see, e.g., Ref. [20]). For the computation of the two-loop ζ_{m_b}, also the one-loop counterterm for the sbottom mixing angle θ_b is required. We adopted the on-shell renormalization prescription as defined in Ref. [44]

$$\delta\theta_b \;=\; \frac{\text{Re}\Sigma_{\tilde{b}_{12}}(m^2_{\tilde{b}_1}) + \text{Re}\Sigma_{\tilde{b}_{12}}(m^2_{\tilde{b}_2})}{2(m^2_{\tilde{b}_1} - m^2_{\tilde{b}_2})}\,, \tag{9}$$

where $\Sigma_{\tilde{b}_{12}}$ is the non-diagonal on-shell sbottom self-energy.

In order to avoid the occurrence of large logarithms of the form $\alpha_s^2 \log(\mu^2/m_b^2)$ with $\mu \simeq \tilde{M}$, we have renormalized the bottom quark mass in the $\overline{\rm DR}$ scheme. In this way, the large logarithms are absorbed into the running mass and the higher order corrections are maintained small.

The renormalization prescription for the trilinear coupling A_b is fixed by the tree-level relation Eq. (8), while the parameters $\mu_{\rm SUSY}$ and $\tan\beta$ do not acquire $\mathcal{O}(\alpha_s)$ corrections to the one-loop level. Generically, the counterterm for A_b can be expressed as

$$\delta A_b = \left(2\cos 2\theta_b \delta\theta_b + \sin 2\theta_b \frac{\delta m^2_{\tilde{b}_1} - \delta m^2_{\tilde{b}_2}}{m^2_{\tilde{b}_1} - m^2_{\tilde{b}_2}} - \sin 2\theta_b \frac{\delta m_b}{m_b} \right) \frac{m^2_{\tilde{b}_1} - m^2_{\tilde{b}_2}}{2 m_b}\,, \tag{10}$$

where δm_b and $\delta m^2_{\tilde{b}_{1,2}}$ are the counterterms corresponding to bottom-quark and squark masses, respectively. Due to the use of different renormalization prescriptions for the bottom/sbottom masses and mixing angle, the parameter A_b is renormalized in a *mixed* scheme.

For the regularization of ultra-violet divergencies, we have implemented DRED with the help of the so-called ϵ-scalars [45]. In softly broken SUSY theories, as it is the case of MSSM/SQCD, they get a radiatively induced mass. We choose to renormalize their mass

in the on-shell scheme, requiring that the renormalized mass is equal to zero.
There are also other approaches available in the literature. We want to mention the one proposed in Ref [46], where the ϵ-scalars are treated as massive particles. This approach is known in the literature as the $\overline{\mathrm{DR}}'$ scheme. In this case, the ϵ-scalars have to be decoupled together with the heavy particles of the theory [37]. The advantage of this method is that it directly relates SQCD parameters regularized within DRED with those of QCD regularized within DREG, which are known from experiments. The price of this "shortcut" is on one hand, that additional diagrams containing the ϵ-scalars as massive particles occur in the calculation of the decoupling coefficients. On the other hand, the contributions originating from the change of regularization scheme and those from the decoupling of heavy particles are not distinguishable anymore.

In our approach the change of regularization scheme from DRED to DREG has to be performed explicitly within QCD [17,18,47]. For our purposes, the two-loop conversion relations for the strong coupling constant and the bottom-quark mass are required. The complication that arises at this stage is the occurrence of the *evanescent coupling* α_e associated with the ϵ-scalar-quark-quark vertex. This has to be distinguished from the gauge coupling within non-supersymmetric theories (e.g. QCD). However, in SQCD they are identical with the gauge couplings, as required by SUSY. Using the ET procedure, we can relate them with the strong coupling within the full theory with the help of decoupling relations similar with those introduced in Eq. (2)

$$\alpha_e' = \zeta_e \alpha_e = \zeta_e \alpha_s \,. \tag{11}$$

Following the method described above, one can calculate ζ_e evaluating the ϵ-scalar and quark-propagators and the ϵ-scalar-quark-quark vertex at vanishing external momentum. In Ref. [23], its one-loop expression was computed under the simplifying assumption of a degenerate SUSY-mass spectrum. In principle, for our numerical analyses, that rely on solving a system of coupled differential equations involving also the evanescent coupling α_e, even the two-loop order corrections to ζ_e are needed. However, from the explicit calculation it turned out that the numerical effects induced by the two-loop corrections to ζ_e are below the per-mille level. For simplicity, we do not display the corresponding two-loop results in the following. The analytical formulae are available upon request from the authors.

The method outlined here and the one introduced in Ref. [37] are equivalent. This has to be understood in the usual sense, that the predictions for physical observables made in one scheme can be translated to the other scheme through redefinitions of masses and couplings. We have explicitly checked the equivalence property for the decoupling coefficient of the bottom-quark mass ζ_m through two-loop order. Apart from the obvious rescaling of the strong coupling and the bottom quark mass, also the sbottom masses have to be modified [46]

$$m_{\tilde{b}}^2|_{\overline{\mathrm{DR}}'} = m_{\tilde{b}}^2|_{\overline{\mathrm{DR}}} - \frac{\alpha_s^{\overline{\mathrm{DR}}}}{2\pi} C_F m_\epsilon^2 \,. \tag{12}$$

Here C_F is the Casimir invariant in the fundamental representation and m_ϵ denotes the mass of the ϵ-scalars. The indices $\overline{\text{DR}}$ and $\overline{\text{DR}}'$, respectively, specify the regularization scheme.

4 Analytical results

4.1 One-loop results

The exact one-loop results for the decoupling coefficients of the strong coupling constant ζ_s and bottom-quark mass ζ_m can be found in Refs. [20, 37]. The analytical formula for ζ_e is new and we give it below up to $\mathcal{O}(\epsilon)$.

$$\begin{aligned}\zeta_s =& 1+\frac{\alpha_s^{(\text{SQCD})}}{\pi}\Bigg[-\frac{1}{6}C_A L_{\tilde{g}}-\frac{1}{6}L_t-\sum_q\sum_{i=1,2}\frac{1}{24}L_{\tilde{q}_i}\\&-\epsilon\left(\frac{C_A}{12}\left(L_{\tilde{g}}^2+\zeta(2)\right)+\frac{1}{12}\left(L_t^2+\zeta(2)\right)-\frac{1}{48}\sum_q\sum_{i=1,2}\left(L_{\tilde{q}_i}^2+\zeta(2)\right)\right)\Bigg],\end{aligned}\tag{13}$$

$$\begin{aligned}\zeta_{e,q} =& 1+\frac{\alpha_s^{(\text{SQCD})}}{\pi}\Bigg\{-T_F\frac{L_t}{2}+\frac{C_A}{4}\left(2+L_{\tilde{g}}+\sum_{i=1,2}\left(L_{\tilde{g}}-L_{\tilde{q}_i}\right)\frac{m_{\tilde{q}_i}^2}{m_{\tilde{g}}^2-m_{\tilde{q}_1}^2}\right)\\&+\frac{C_F}{4}\left(\sum_{i=1,2}\left(-1-2L_{\tilde{g}}+2L_{\tilde{q}_i}+\left(-L_{\tilde{g}}+L_{\tilde{q}_i}\right)\frac{m_{\tilde{q}_i}^2}{m_{\tilde{g}}^2-m_{\tilde{q}_i}^2}\right)\frac{m_{\tilde{q}_i}^2}{m_{\tilde{g}}^2-m_{\tilde{q}_i}^2}\right.\\&\left.+\left(-3-2L_{\tilde{g}}\right)\right)+\epsilon\Bigg[-\frac{T_F}{4}\left(L_t^2+\zeta(2)\right)+\frac{C_A}{8}\Bigg(4+4L_{\tilde{g}}+L_{\tilde{g}}^2+\zeta(2)+\\&+\frac{1}{2}\sum_{i=1,2}\left(L_{\tilde{g}}-L_{\tilde{q}_i}\right)\left(2+L_{\tilde{g}}+L_{\tilde{q}_i}\right)\frac{m_{\tilde{q}_i}^2}{m_{\tilde{g}}^2-m_{\tilde{q}_i}^2}\Bigg)+\frac{C_F}{8}\Bigg(-7-6L_{\tilde{g}}-2L_{\tilde{g}}^2\\&-2\zeta(2)+\frac{1}{2}\sum_{i=1,2}\Bigg(-3-6L_{\tilde{g}}-2L_{\tilde{g}}^2+4L_{\tilde{q}_i}+2L_{\tilde{q}_i}^2\\&-\left(L_{\tilde{g}}-L_{\tilde{q}_1}\right)\left(3+L_{\tilde{g}}+L_{\tilde{q}_1}\right)\frac{m_{\tilde{q}_i}^2}{m_{\tilde{g}}^2-m_{\tilde{q}_i}^2}\Bigg)\frac{m_{\tilde{q}_i}^2}{m_{\tilde{g}}^2-m_{\tilde{q}_i}^2}\Bigg)\Bigg]\Bigg\},\end{aligned}\tag{14}$$

$$\begin{aligned}\zeta_{m_b} =& 1+\frac{\alpha_s^{(\text{SQCD})}}{\pi}C_F\sum_{i=1,2}\Bigg\{-\frac{(1+L_{\tilde{b}_i})}{4}\frac{m_{\tilde{b}_i}^2}{(m_{\tilde{b}_i}^2-m_{\tilde{g}}^2)}+\frac{(3+2L_{\tilde{b}_i})m_{\tilde{b}_i}^4-(3+2L_{\tilde{g}})m_{\tilde{g}}^4}{16(m_{\tilde{b}_i}^2-m_{\tilde{g}}^2)^2}\\&-\frac{(-1)^i X_b m_{\tilde{g}}}{m_{\tilde{b}_1}^2-m_{\tilde{b}_2}^2}\frac{m_{\tilde{b}_i}^2 L_{\tilde{b}_i}-m_{\tilde{g}}^2 L_{\tilde{g}}}{2(m_{\tilde{b}_i}^2-m_{\tilde{g}}^2)}+\epsilon\Bigg[-\frac{m_{\tilde{b}_i}^2(2+L_{\tilde{b}_i}(2+L_{\tilde{b}_i})+\zeta(2))}{8(m_{\tilde{b}_i}^2-m_{\tilde{g}}^2)}\\&+\frac{m_{\tilde{b}_i}^4(7+2L_{\tilde{b}_i}(3+L_{\tilde{b}_i})+2\zeta(2))-m_{\tilde{g}}^4(7+2L_{\tilde{g}}(3+L_{\tilde{g}})+2\zeta(2))}{32(m_{\tilde{b}_i}^2-m_{\tilde{g}}^2)^2}\end{aligned}$$

$$+\frac{(-1)^i X_b m_{\tilde{g}}}{m^2_{\tilde{b}_1}-m^2_{\tilde{b}_2}}\frac{m^2_{\tilde{g}}L_{\tilde{g}}(2+L_{\tilde{g}})-m^2_{\tilde{b}_i}L_{\tilde{b}_i}(2+L_{\tilde{b}_i})}{4(m^2_{\tilde{b}_i}-m^2_{\tilde{g}})}\Bigg]\Bigg\}\,. \tag{15}$$

In Eqs. (13), (14), and (15), we have adopted the abbreviations

$$L_i=\ln\frac{\mu^2}{m_i^2}\,,\quad i\in\{t,\tilde{g},\tilde{q}_{1,2},\tilde{b}_{1,2}\}\,, \tag{16}$$

where $\tilde{q}_i(\tilde{b}_i)$ denote the super-partners of the quark $q(b)$. For our purposes, the special case $\zeta_{e,q=b}$ is of interest.
The colour factors are defined in case of a gauge group $SU(N)$ as follows

$$C_F=\frac{N^2-1}{2N}\quad C_A=N\,,\quad T_F=\frac{1}{2}\,. \tag{17}$$

Furthermore, we used the notation $\zeta(2)=\pi^2/6$ and introduced the label "SQCD" to specify that the strong coupling has to be evaluated within the full theory, i.e. the SQCD with $n_f=n_s=6$ active flavours.

The presence of the terms proportional with the parameter X_b is a manifestation of the supersymmetry breaking. They are generated by the Yukawa interaction between left- and right-handed bottom squarks and the CP-neutral Higgs fields. Their contribution to the decoupling coefficient of the bottom-quark mass can be related through the Low Energy Theorem [48] to the decay rate of the Higgs boson to $b\bar{b}$ pairs. To one-loop order, the X_b-term of Eq. (15) coincides with the SQCD corrections to the decay rate $\phi\to b\bar{b}$ [49]. To higher orders, the relation between the two parameters becomes more involved.
The Yukawa-coupling induced contributions attracted a lot of attention in the past years, due to the fact that they are the dominant corrections for large values of $\tan\beta$. They may in general become comparable with the tree-level bottom-quark mass. The resummation of the one-loop corrections was performed in Ref. [28].

4.2 Two-loop calculation

The analytical two-loop results for the decoupling coefficients are too lengthy to be displayed here. They are available in `MATHEMATICA` format from http://www-ttp.particle.uni-karlsruhe.de/Progdata/ttp08-25. Instead, we present the two-loop results for three special cases of the hierarchy among the heavy particle masses. Before displaying the analytical results, let us notice the absence of contributions of the form $\alpha_s^2X_b^2$ to ζ_{m_b}, in accordance with Refs. [28, 49]. They are suppressed by a factor $m_b/\tilde{M}$, that we neglect in the ET formalism.

4.2.1 Scenario A

We consider first the case of all supersymmetric particles having masses of the same order of magnitude and being much heavier than the top-quark

$$
\begin{aligned}
m_{\tilde{u}} = \ldots = m_{\tilde{b}} = m_{\tilde{t}} = m_{\tilde{g}} = \tilde{M} \quad &\gg \quad m_t \\
\alpha_s^{(5)} = \zeta_s^{\tilde{M}}\, \alpha_s^{(\mathrm{SQCD})}\,, \qquad & m_b^{(5)} = \zeta_{m_b}^{\tilde{M}}\, m_b^{(\mathrm{SQCD})}\,.
\end{aligned}
$$

$\zeta_s^{\tilde{M}}$, $\zeta_{m_b}^{\tilde{M}}$ are functions of the supersymmetric mass $\tilde{M}$ and the top-quark mass m_t, the soft SUSY breaking parameters X_q, $q = b, t$, the strong coupling constant in the full theory $\alpha_s^{(\mathrm{SQCD})}$ and the decoupling scale μ. The superscript (5) indicates that the parameters are defined in QCD with $n_l = 5$ light quarks. In addition to the notations introduced in Eq. (16), the following abbreviation will be used

$$
L_{\tilde{M}} = \ln \frac{\mu^2}{\tilde{M}^2}\,. \tag{18}
$$

The two-loop result for the decoupling coefficient of α_s in case of a degenerate SUSY mass spectrum is known [22], however we give it here for completeness

$$
\begin{aligned}
\zeta_s^{\tilde{M}} = 1 &+ \frac{\alpha_s^{(\mathrm{SQCD})}}{\pi}\left[C_A\left(-\frac{1}{6}L_{\tilde{M}}\right) + \left(-L_{\tilde{M}} - \frac{L_t}{3}\right)T_F\right] + \left(\frac{\alpha_s^{(\mathrm{SQCD})}}{\pi}\right)^2\Bigg\{C_A^2\Bigg(-\frac{85}{288} \\
&- \frac{L_{\tilde{M}}}{3} + \frac{L_{\tilde{M}}^2}{36}\Bigg) + C_F T_F\Bigg[-\frac{31}{16} - \frac{3L_{\tilde{M}}}{2} - \frac{L_t}{4} - \frac{m_t^2}{8\tilde{M}^2} + \frac{\pi m_t^3}{12\tilde{M}^3} + \Bigg(-\frac{17}{150} - \frac{3L_{\tilde{M}}}{40} \\
&+ \frac{3L_t}{40}\Bigg)\frac{m_t^4}{\tilde{M}^4}\Bigg] + C_A T_F\Bigg[\frac{41}{36} + L_{\tilde{M}} + \frac{L_{\tilde{M}}^2}{3} - \frac{5L_t}{12} + \frac{L_{\tilde{M}}L_t}{9} + \left(\frac{1}{8} + \frac{L_{\tilde{M}}}{4} - \frac{L_t}{4}\right)\frac{m_t^2}{m_S^2} \\
&- \frac{\pi m_t^3}{6\tilde{M}^3} + \left(\frac{19}{144} + \frac{L_{\tilde{M}}}{24} - \frac{L_t}{24}\right)\frac{m_t^4}{\tilde{M}^4}\Bigg] + T_F^2\left(L_{\tilde{M}}^2 + \frac{2L_{\tilde{M}}L_t}{3} + \frac{L_t^2}{9}\right) \\
&+ \mathcal{O}\left(\frac{m_t^5}{\tilde{M}^5}\right)\Bigg\}\,,
\end{aligned} \tag{19}
$$

$$
\begin{aligned}
\zeta_{m_b}^{\tilde{M}} = 1 &- \frac{\alpha_s^{(\mathrm{SQCD})}}{\pi}C_F\left[\frac{L_{\tilde{M}}}{4} + \frac{X_b}{4\tilde{M}}\right] + \left(\frac{\alpha_s^{(\mathrm{SQCD})}}{\pi}\right)^2 C_F\Bigg\{-C_A\left(\frac{65}{1152} + \frac{43L_{\tilde{M}}}{96} + \frac{L_{\tilde{M}}^2}{32}\right) \\
&+ C_F\left(-\frac{99}{128} - \frac{7L_{\tilde{M}}}{32} + \frac{L_{\tilde{M}}^2}{32}\right) + T_F\Bigg[\frac{197}{72} - L_{\tilde{M}} + \frac{3L_{\tilde{M}}^2}{4} - \frac{L_t}{12} + \frac{L_t^2}{8} \\
&+ \left(\frac{7}{144} + \frac{L_{\tilde{M}}}{12} - \frac{L_t}{12}\right)\frac{m_t^2}{\tilde{M}^2} - \frac{\pi}{12}\frac{m_t^3}{\tilde{M}^3} + \left(\frac{53}{600} - \frac{7L_{\tilde{M}}}{160} + \frac{7L_t}{160}\right)\frac{m_t^4}{\tilde{M}^4}\Bigg] \\
&+ \frac{X_b}{\tilde{M}}\Bigg[-C_A\left(\frac{1}{16} + \frac{3L_{\tilde{M}}}{16}\right) - C_F\left(\frac{1}{4} - \frac{3L_{\tilde{M}}}{16}\right) + T_F\Bigg[\frac{-3}{4} + \frac{3L_{\tilde{M}}}{4}
\end{aligned}
$$

$$+\left(\frac{-7}{72}-\frac{L_{\tilde{M}}}{24}+\frac{L_t}{24}\right)\frac{m_t^2}{\tilde{M}^2}+\frac{\pi}{24}\frac{m_t^3}{\tilde{M}^3}+\left(-\frac{17}{450}+\frac{L_{\tilde{M}}}{240}-\frac{L_t}{240}\right)\frac{m_t^4}{\tilde{M}^4}\Big]\Big]$$
$$+\frac{X_t}{\tilde{M}}T_F\left[\left(\frac{-5}{72}+\frac{L_{\tilde{M}}}{12}-\frac{L_t}{12}\right)\frac{m_t^2}{\tilde{M}^2}-\frac{\pi}{24}\frac{m_t^3}{\tilde{M}^3}+\left(\frac{23}{450}-\frac{L_{\tilde{M}}}{60}+\frac{L_t}{60}\right)\frac{m_t^4}{\tilde{M}^4}\right]$$
$$+\frac{X_tX_b}{\tilde{M}^2}T_F\left[\left(\frac{1}{72}-\frac{L_{\tilde{M}}}{24}+\frac{L_t}{24}\right)\frac{m_t^2}{\tilde{M}^2}+\frac{\pi}{48}\frac{m_t^3}{\tilde{M}^3}+\left(\frac{-59}{1800}-\frac{L_{\tilde{M}}}{120}+\frac{L_t}{120}\right)\frac{m_t^4}{\tilde{M}^4}\right]$$
$$+\mathcal{O}\left(\frac{m_t^5}{\tilde{M}^5}\right)\Bigg\}. \tag{20}$$

Let us point out that, according to Eq. (8) the assumption of degenerate top-squark masses can be materialized only if $X_t \to 0$, due to the heavy top-quark mass. We display, however, for completeness the full result. Further on, the hypothesis of equal top- and bottom-squark masses is inconsistent with the $SU(2)$ invariance of the $\tilde{t}/\tilde{b}$ isodublet imposed in models like mSUGRA.

4.2.2 Scenario B

In the following, we discuss the possibility that the gluino is the heaviest supersymmetric particle and the squarks have equal masses, much heavier than that of the top-quark

$$\begin{array}{l} m_{\tilde{g}} \quad \gg \quad m_{\tilde{u}} = \ldots = m_{\tilde{b}} = m_{\tilde{t}} = m_{\tilde{q}} \quad \gg \quad m_t \\ \alpha_s^{(5)} = \zeta_s^{\tilde{g}}\,\alpha_s^{(\mathrm{SQCD})}\,, \qquad m_b^{(5)} = \zeta_{m_b}^{\tilde{g}}\,m_b^{(\mathrm{SQCD})}\,. \end{array}$$

The two-loop results read

$$\zeta_s^{\tilde{g}} = 1+\frac{\alpha_s^{(\mathrm{SQCD})}}{\pi}\left[C_A\left(-\frac{1}{6}L_{\tilde{g}}\right)+\left(-\frac{L_t}{3}-L_{\tilde{q}}\right)T_F\right]+\left(\frac{\alpha_s^{(\mathrm{SQCD})}}{\pi}\right)^2\Bigg\{C_A^2\left(-\frac{85}{288}-\frac{L_{\tilde{g}}}{3}\right.$$
$$\left.+\frac{L_{\tilde{g}}^2}{36}\right)+T_F^2\left(\frac{L_t^2}{9}+\frac{2}{3}L_tL_{\tilde{q}}+L_{\tilde{q}}^2\right)+C_FT_F\Bigg[-\frac{19}{16}-\frac{L_t}{4}+\frac{3L_{\tilde{g}}}{2}-3L_{\tilde{q}}+\left(\frac{1}{6}+L_{\tilde{g}}\right.$$
$$\left.-L_{\tilde{q}}\right)\frac{m_{\tilde{q}}^2}{m_{\tilde{g}}^2}+\left(\frac{1}{24}+L_{\tilde{g}}-L_{\tilde{q}}\right)\frac{m_{\tilde{q}}^4}{m_{\tilde{g}}^4}+\left(-\frac{5}{9}+\frac{L_t}{3}-\frac{L_{\tilde{g}}}{3}\right)\frac{m_t^2}{m_{\tilde{g}}^2}+\left(-\frac{9}{8}+\frac{5L_t}{4}-\frac{5L_{\tilde{g}}}{4}\right)\frac{m_t^4}{m_{\tilde{g}}^4}$$
$$+\frac{m_t^2m_{\tilde{q}}^2}{m_{\tilde{g}}^4}\left(-\frac{41}{36}+\frac{11L_t}{6}-\frac{23L_{\tilde{g}}}{6}+L_tL_{\tilde{g}}-L_{\tilde{g}}^2+2L_{\tilde{q}}-L_tL_{\tilde{q}}+L_{\tilde{g}}L_{\tilde{q}}-2\zeta_2\right)\Bigg]$$
$$+C_AT_F\Bigg[\frac{95}{36}-\frac{5L_t}{12}+\frac{3L_{\tilde{g}}}{2}+\frac{1}{9}L_tL_{\tilde{g}}-\frac{L_{\tilde{q}}}{2}+\frac{1}{3}L_{\tilde{g}}L_{\tilde{q}}+\left(-\frac{3L_{\tilde{g}}}{2}+\frac{3L_{\tilde{q}}}{2}\right)\frac{m_{\tilde{q}}^2}{m_{\tilde{g}}^2}$$
$$+\left(-\frac{3}{2}+\frac{3L_{\tilde{g}}}{2}-\frac{3L_{\tilde{q}}}{2}\right)\frac{m_{\tilde{q}}^4}{m_{\tilde{g}}^4}+\left(\frac{1}{2}-\frac{L_t}{4}+\frac{L_{\tilde{g}}}{4}\right)\frac{m_t^2}{m_{\tilde{g}}^2}+\left(\frac{1}{4}-\frac{L_t}{4}+\frac{L_{\tilde{g}}}{4}\right)\frac{m_t^4}{m_{\tilde{g}}^4}$$

$$+\frac{m_t^2 m_{\tilde{q}}^2}{m_{\tilde{g}}^4}\left(\frac{1}{2}-\frac{3L_t}{4}+\frac{3L_{\tilde{g}}}{2}-\frac{1}{2}L_tL_{\tilde{g}}+\frac{L_{\tilde{g}}^2}{2}-\frac{3L_{\tilde{q}}}{4}+\frac{1}{2}L_tL_{\tilde{q}}-\frac{1}{2}L_{\tilde{g}}L_{\tilde{q}}+\zeta_2\right)\Bigg]$$

$$+\mathcal{O}\left(\frac{m_{\tilde{q}}^6}{m_{\tilde{g}}^6},\frac{m_{\tilde{q}}^4 m_t^2}{m_{\tilde{g}}^6},\frac{m_{\tilde{q}}^2 m_t^4}{m_{\tilde{g}}^6},\frac{m_t^6}{m_{\tilde{g}}^6}\right)\Bigg\}, \tag{21}$$

$$\zeta_{m_b}^{\tilde{g}}=1+\frac{\alpha_s^{(\mathrm{SQCD})}}{\pi}C_F\Bigg\{-\frac{3}{8}-\frac{L_{\tilde{g}}}{4}+\left(-\frac{1}{4}-\frac{L_{\tilde{g}}}{2}+\frac{L_{\tilde{q}}}{2}\right)\frac{m_{\tilde{q}}^2}{m_{\tilde{g}}^2}+\left(-\frac{1}{4}-\frac{3L_{\tilde{g}}}{4}+\frac{3L_{\tilde{q}}}{4}\right)\frac{m_{\tilde{q}}^4}{m_{\tilde{g}}^4}$$

$$+\frac{X_b}{m_{\tilde{g}}}\left[\frac{1}{2}+\frac{L_{\tilde{g}}}{2}-\frac{L_{\tilde{q}}}{2}+\left(\frac{1}{2}+L_{\tilde{g}}-L_{\tilde{q}}\right)\frac{m_{\tilde{q}}^2}{m_{\tilde{g}}^2}+\left(\frac{1}{2}+\frac{3L_{\tilde{g}}}{2}-\frac{3L_{\tilde{q}}}{2}\right)\frac{m_{\tilde{q}}^4}{m_{\tilde{g}}^4}\right]\Bigg\}$$

$$+\left(\frac{\alpha_s^{(\mathrm{SQCD})}}{\pi}\right)^2 C_F\Bigg\{C_A\Bigg[-\frac{209}{1152}-\frac{35L_{\tilde{g}}}{48}-\frac{L_{\tilde{g}}^2}{32}-\frac{\zeta(2)}{8}+\Bigg(-\frac{5}{16}-\frac{3L_{\tilde{g}}}{2}-\frac{5L_{\tilde{g}}^2}{8}$$

$$+\frac{21L_{\tilde{q}}}{16}+\frac{7L_{\tilde{g}}L_{\tilde{q}}}{8}-\frac{L_{\tilde{q}}^2}{4}-\frac{5\zeta(2)}{8}\Bigg)\frac{m_{\tilde{q}}^2}{m_{\tilde{g}}^2}+\Bigg(\frac{7}{32}-\frac{11L_{\tilde{g}}}{4}-\frac{37L_{\tilde{g}}^2}{32}+\frac{41L_{\tilde{q}}}{16}+\frac{7L_{\tilde{g}}L_{\tilde{q}}}{4}-\frac{19L_{\tilde{q}}^2}{32}$$

$$-\frac{5\zeta(2)}{8}\Bigg)\frac{m_{\tilde{q}}^4}{m_{\tilde{g}}^4}\Bigg]+C_F\Bigg[-\frac{221}{128}-\frac{L_{\tilde{g}}}{8}+\frac{L_{\tilde{g}}^2}{32}-\frac{\zeta(2)}{16}+\Bigg(\frac{9}{16}+\frac{5L_{\tilde{g}}^2}{8}+\frac{L_{\tilde{q}}}{16}-\frac{9L_{\tilde{g}}L_{\tilde{q}}}{8}$$

$$+\frac{L_{\tilde{q}}^2}{2}+\frac{\zeta(2)}{2}\Bigg)\frac{m_{\tilde{q}}^2}{m_{\tilde{g}}^2}+\Bigg(\frac{31}{192}+\frac{35L_{\tilde{g}}}{32}+\frac{17L_{\tilde{g}}^2}{16}-\frac{33L_{\tilde{q}}}{32}-\frac{31L_{\tilde{g}}L_{\tilde{q}}}{16}+\frac{7L_{\tilde{q}}^2}{8}+\frac{\zeta(2)}{8}\Bigg)\frac{m_{\tilde{q}}^4}{m_{\tilde{g}}^4}\Bigg]$$

$$+T_F\Bigg[\frac{139}{36}+\frac{3L_{\tilde{g}}}{2}+\frac{3L_{\tilde{g}}^2}{8}-\frac{11L_{\tilde{q}}}{8}+\frac{3L_{\tilde{q}}^2}{8}-\frac{L_t}{12}+\frac{L_t^2}{8}+\frac{3\zeta(2)}{4}$$

$$+\left(3+\frac{9L_{\tilde{g}}}{2}+3L_{\tilde{g}}^2-\frac{15L_{\tilde{q}}}{4}-\frac{9L_{\tilde{g}}L_{\tilde{q}}}{2}+\frac{3L_{\tilde{q}}^2}{2}\right)\frac{m_{\tilde{q}}^2}{m_{\tilde{g}}^2}+\left(-\frac{1}{2}-\frac{L_{\tilde{g}}}{4}+\frac{L_{\tilde{q}}}{4}\right)\frac{m_t^2}{m_{\tilde{g}}^2}$$

$$-\left(1+\frac{L_{\tilde{g}}}{2}-\frac{3L_{\tilde{g}}^2}{8}-\frac{L_{\tilde{q}}}{2}+\frac{3L_{\tilde{g}}L_{\tilde{q}}}{4}-\frac{3L_{\tilde{q}}^2}{8}-\frac{3\zeta(2)}{4}\right)\frac{m_{\tilde{q}}^2 m_t^2}{m_{\tilde{g}}^4}$$

$$+\left(-\frac{5}{72}+\frac{L_{\tilde{q}}}{24}-\frac{L_t}{24}\right)\frac{m_t^4}{m_{\tilde{q}}^2 m_{\tilde{g}}^2}+\Bigg(-\frac{155}{96}-\frac{3L_{\tilde{g}}}{16}+\frac{3L_{\tilde{g}}^2}{16}+\frac{7L_{\tilde{q}}}{8}-\frac{3L_{\tilde{q}}^2}{16}-\frac{11L_t}{16}$$

$$-\frac{3L_{\tilde{g}}L_t}{8}+\frac{3L_{\tilde{q}}L_t}{8}+\frac{3\zeta(2)}{8}\Bigg)\frac{m_t^4}{m_{\tilde{g}}^4}+\left(\frac{69}{16}+\frac{63L_{\tilde{g}}}{8}+3L_{\tilde{g}}^2-\frac{57L_{\tilde{q}}}{8}-\frac{15L_{\tilde{g}}L_{\tilde{q}}}{4}+\frac{3L_{\tilde{q}}^2}{4}\right)\frac{m_{\tilde{q}}^4}{m_{\tilde{g}}^4}\Bigg]$$

$$+\frac{X_b}{m_{\tilde{g}}}\Bigg[C_A\Bigg[\frac{7}{8}+L_{\tilde{g}}+\frac{3L_{\tilde{g}}^2}{8}-\frac{5L_{\tilde{q}}}{8}-\frac{3L_{\tilde{g}}L_{\tilde{q}}}{8}-\frac{\zeta(2)}{4}+\Bigg(\frac{9}{8}+\frac{17L_{\tilde{g}}}{8}+\frac{11L_{\tilde{g}}^2}{8}-\frac{7L_{\tilde{q}}}{4}$$

$$-2L_{\tilde{g}}L_{\tilde{q}}+\frac{5L_{\tilde{q}}^2}{8}-\frac{\zeta(2)}{4}\Bigg)\frac{m_{\tilde{q}}^2}{m_{\tilde{g}}^2}+\Bigg(\frac{19}{16}+\frac{27L_{\tilde{g}}}{8}+\frac{23L_{\tilde{g}}^2}{8}-3L_{\tilde{q}}-\frac{37L_{\tilde{g}}L_{\tilde{q}}}{8}+\frac{7L_{\tilde{q}}^2}{4}$$

$$-\frac{\zeta(2)}{4}\Bigg)\frac{m_{\tilde{q}}^4}{m_{\tilde{g}}^4}\Bigg]+C_F\Bigg[\frac{1}{16}-\frac{3L_{\tilde{g}}}{16}-\frac{3L_{\tilde{g}}^2}{8}-\frac{3L_{\tilde{q}}}{16}+\frac{3L_{\tilde{g}}L_{\tilde{q}}}{8}+\frac{\zeta(2)}{2}+\Bigg(-\frac{9}{16}-\frac{5L_{\tilde{g}}}{24}$$

$$-\frac{3L_{\tilde{g}}^2}{2}-\frac{L_{\tilde{q}}}{6}+\frac{9L_{\tilde{g}}L_{\tilde{q}}}{4}-\frac{3L_{\tilde{q}}^2}{4}+\frac{\zeta(2)}{2}\Bigg)\frac{m_{\tilde{q}}^2}{m_{\tilde{g}}^2}+\Bigg(-\frac{13}{16}-\frac{3L_{\tilde{g}}}{4}-\frac{13L_{\tilde{g}}^2}{4}+\frac{3L_{\tilde{q}}}{8}$$

$$
\begin{aligned}
&+\frac{43L_{\tilde g}L_{\tilde q}}{8}-\frac{17L_{\tilde q}^2}{8}+\frac{\zeta(2)}{2}\bigg)\frac{m_{\tilde q}^4}{m_{\tilde g}^4}\bigg]+T_F\bigg[-\frac{3}{2}(2+L_{\tilde g})(1+L_{\tilde g}-L_{\tilde q})+\bigg(-9-\frac{15L_{\tilde g}}{2}\\
&-6L_{\tilde g}^2+6L_{\tilde q}+9L_{\tilde g}L_{\tilde q}-3L_{\tilde q}^2\bigg)\frac{m_{\tilde q}^2}{m_{\tilde g}^2}+\bigg(\frac{3}{2}+\frac{L_{\tilde g}}{2}-\frac{L_{\tilde q}}{2}\bigg)\frac{m_t^2}{m_{\tilde g}^2}+\bigg(-\frac{33}{4}-\frac{63L_{\tilde g}}{4}-6L_{\tilde g}^2\\
&+\frac{57L_{\tilde q}}{4}+\frac{15L_{\tilde g}L_{\tilde q}}{2}-\frac{3L_{\tilde q}^2}{2}\bigg)\frac{m_{\tilde q}^4}{m_{\tilde g}^4}+\bigg(\frac{5}{18}-\frac{L_{\tilde q}}{6}+\frac{L_t}{6}\bigg)\frac{m_t^4}{m_{\tilde q}^2m_{\tilde g}^2}\\
&+\bigg(\frac{5}{2}+\frac{3L_{\tilde g}}{2}-\frac{L_{\tilde g}^2}{2}-\frac{3L_{\tilde q}}{2}+L_{\tilde g}L_{\tilde q}-\frac{L_{\tilde q}^2}{2}-2\zeta(2)\bigg)\frac{m_t^2m_{\tilde q}^2}{m_{\tilde g}^4}\\
&+\bigg(\frac{301}{72}+\frac{5L_{\tilde g}}{8}-\frac{L_{\tilde g}^2}{4}-\frac{53L_{\tilde q}}{24}-\frac{L_{\tilde g}L_{\tilde q}}{4}+\frac{L_{\tilde q}^2}{2}+\frac{19L_t}{12}+\frac{3L_{\tilde g}L_t}{4}-\frac{3L_{\tilde q}L_t}{4}-\zeta(2)\bigg)\frac{m_t^4}{m_{\tilde g}^4}\bigg]\bigg]\\
&+\frac{X_t}{m_{\tilde g}}T_F\bigg[\bigg(\frac{1}{2}-L_{\tilde g}-\frac{L_{\tilde g}^2}{4}+L_{\tilde q}+\frac{L_{\tilde g}L_{\tilde q}}{2}-\frac{L_{\tilde q}^2}{4}-\frac{\zeta(2)}{2}\bigg)\frac{m_t^2}{m_{\tilde g}^2}+\bigg(1-\frac{7L_{\tilde g}}{2}-2L_{\tilde g}^2+\frac{7L_{\tilde q}}{2}\\
&+4L_{\tilde g}L_{\tilde q}-2L_{\tilde q}^2-2\zeta(2)\bigg)\frac{m_t^2m_{\tilde q}^2}{m_{\tilde g}^4}+\bigg(\frac{4}{9}-\frac{L_{\tilde q}}{6}+\frac{L_t}{6}\bigg)\frac{m_t^4}{m_{\tilde g}^2m_{\tilde q}^2}+\bigg(\frac{17}{9}-3L_{\tilde g}-L_{\tilde g}^2+\frac{L_{\tilde q}}{6}\\
&+L_{\tilde g}L_{\tilde q}+\frac{17L_t}{6}+L_{\tilde g}L_t-L_{\tilde q}L_t-2\zeta(2)\bigg)\frac{m_t^4}{m_{\tilde g}^4}\bigg]+\frac{X_tX_b}{m_{\tilde g}^2}T_F\bigg[-\frac{1}{2}\frac{m_t^2}{m_{\tilde q}^2}+\bigg(-\frac{3}{2}+\frac{5L_{\tilde g}}{2}\\
&+\frac{5L_{\tilde g}^2}{4}-\frac{5L_{\tilde q}}{2}-\frac{5L_{\tilde g}L_{\tilde q}}{2}+\frac{5L_{\tilde q}^2}{4}+\frac{3\zeta(2)}{2}\bigg)\frac{m_t^2}{m_{\tilde g}^2}\bigg]+\mathcal{O}\left(\frac{m_{\tilde q}^6}{m_{\tilde g}^6},\frac{m_{\tilde q}^4m_t^2}{m_{\tilde g}^6},\frac{m_{\tilde q}^2m_t^4}{m_{\tilde g}^6},\frac{m_t^6}{m_{\tilde g}^6},\frac{X_tX_bm_t^4}{m_{\tilde g}^6}\right)\bigg\}\,.
\end{aligned}
\tag{22}
$$

4.2.3 Scenario C

Finally, we make the assumption that all squark masses are degenerate and are much heavier than the gluino and top masses

$$
\begin{aligned}
&m_{\tilde u}=\ldots=m_{\tilde b}=m_{\tilde t}=m_{\tilde q}\quad\gg\quad m_{\tilde g}\quad\gg\quad m_t\\
&\alpha_s^{(5)}=\zeta_s^{\tilde q}\,\alpha_s^{(\mathrm{SQCD})}\,,\qquad m_b^{(5)}=\zeta_{m_b}^{\tilde q}\,m_b^{(\mathrm{SQCD})}\,.
\end{aligned}
$$

The decoupling coefficients are given by

$$
\begin{aligned}
\zeta_s^{\tilde q}\;=\;&1+\frac{\alpha_s^{(\mathrm{SQCD})}}{\pi}\bigg[-\frac{1}{6}C_AL_{\tilde g}+\bigg(-\frac{L_t}{3}-L_{\tilde q}\bigg)T_F\bigg]+\bigg(\frac{\alpha_s^{(\mathrm{SQCD})}}{\pi}\bigg)^2\bigg\{C_A^2\bigg(-\frac{85}{288}-\frac{L_{\tilde g}}{3}\\
+\;&\frac{L_{\tilde g}^2}{36}\bigg)+C_FT_F\bigg[-\frac{7}{16}-\frac{L_t}{4}-\frac{3L_{\tilde q}}{2}+\bigg(-\frac{1}{9}-\frac{L_t}{12}+\frac{L_{\tilde q}}{12}\bigg)\frac{m_t^4}{m_{\tilde q}^4}+\bigg(-\frac{1}{9}-\frac{L_t}{3}\\
+\;&\frac{L_{\tilde q}}{3}\bigg)\frac{m_t^2m_{\tilde g}^2}{m_{\tilde q}^4}+\bigg(-\frac{3}{4}-\frac{3L_{\tilde g}}{2}+\frac{3L_{\tilde q}}{2}\bigg)\frac{m_{\tilde g}^4}{m_{\tilde q}^4}+\bigg(\frac{1}{18}+\frac{L_t}{6}-\frac{L_{\tilde q}}{6}\bigg)\frac{m_t^2}{m_{\tilde q}^2}\bigg]+T_F^2\bigg(\frac{L_t^2}{9}
\end{aligned}
$$

$$
\begin{aligned}
&+ \frac{2}{3}L_tL_{\tilde{q}} + L_{\tilde{q}}^2\Bigg) + C_AT_F\Bigg[\frac{41}{36} - \frac{5L_t}{12} + \frac{1}{9}L_tL_{\tilde{g}} + L_{\tilde{q}} + \frac{1}{3}L_{\tilde{g}}L_{\tilde{q}} + \Bigg(-\frac{L_t}{4} + \frac{L_{\tilde{q}}}{4}\Bigg)\frac{m_t^2}{m_{\tilde{q}}^2} \\
&+ \Bigg(\frac{1}{3} - \frac{L_{\tilde{g}}}{2} + \frac{L_{\tilde{q}}}{2}\Bigg)\frac{m_{\tilde{g}}^2}{m_{\tilde{q}}^2} + \Bigg(-\frac{L_t}{4} + \frac{L_{\tilde{q}}}{4}\Bigg)\frac{m_t^4}{m_{\tilde{q}}^4} + \Bigg(\frac{1}{12} - \frac{L_{\tilde{g}}}{2} + \frac{L_{\tilde{q}}}{2}\Bigg)\frac{m_{\tilde{g}}^4}{m_{\tilde{q}}^4} \\
&+ \frac{m_t^2m_{\tilde{g}}^2}{m_{\tilde{q}}^4}\Bigg(\frac{7}{18} - \frac{3L_t}{4} - \frac{13L_{\tilde{g}}}{12} + \frac{1}{2}L_tL_{\tilde{g}} + \frac{11L_{\tilde{q}}}{6} - \frac{1}{2}L_tL_{\tilde{q}} - \frac{1}{2}L_{\tilde{g}}L_{\tilde{q}} + \frac{L_{\tilde{q}}^2}{2} + \zeta_2\Bigg)\Bigg] \\
&+ \mathcal{O}\left(\frac{m_{\tilde{g}}^6}{m_{\tilde{q}}^6}, \frac{m_{\tilde{g}}^4m_t^2}{m_{\tilde{q}}^6}, \frac{m_{\tilde{g}}^2m_t^4}{m_{\tilde{q}}^6}, \frac{m_t^6}{m_{\tilde{q}}^6}\right)\Bigg\}, \qquad (23)
\end{aligned}
$$

$$
\begin{aligned}
\zeta_{m_b}^{\tilde{q}} &= 1 + \frac{\alpha_s^{(\mathrm{SQCD})}}{\pi}C_F\Bigg\{-\frac{1}{8} - \frac{L_{\tilde{q}}}{4} + \frac{m_{\tilde{g}}^2}{4m_{\tilde{q}}^2} + \Bigg(\frac{1}{4} - \frac{L_{\tilde{g}}}{4} + \frac{L_{\tilde{q}}}{4}\Bigg)\frac{m_{\tilde{g}}^4}{m_{\tilde{q}}^4} + \frac{X_b}{m_{\tilde{q}}}\Bigg[-\frac{m_{\tilde{g}}}{2m_{\tilde{q}}} \\
&+ \Bigg(-\frac{1}{2} + \frac{L_{\tilde{g}}}{2} - \frac{L_{\tilde{q}}}{2}\Bigg)\frac{m_{\tilde{g}}^3}{m_{\tilde{q}}^3}\Bigg]\Bigg\} + \Bigg(\frac{\alpha_s^{(\mathrm{SQCD})}}{\pi}\Bigg)^2 C_F\Bigg\{C_A\Bigg[\frac{295}{1152} - \frac{L_{\tilde{g}}}{24} + \frac{L_{\tilde{g}}^2}{16} - \frac{L_{\tilde{q}}}{2} - \frac{3L_{\tilde{q}}^2}{32} \\
&- \frac{\zeta(2)}{2} + \Bigg(\frac{15}{16} + \frac{L_{\tilde{g}}}{2} - \frac{5L_{\tilde{q}}}{16} - \frac{5\zeta(2)}{8}\Bigg)\frac{m_{\tilde{g}}^2}{m_{\tilde{q}}^2} + \Bigg(\frac{19}{16} + \frac{3L_{\tilde{g}}}{16} + \frac{7L_{\tilde{g}}^2}{32} + \frac{13L_{\tilde{q}}^2}{32} - \frac{5L_{\tilde{g}}L_{\tilde{q}}}{8} \\
&- \frac{5\zeta(2)}{8}\Bigg)\frac{m_{\tilde{g}}^4}{m_{\tilde{q}}^4}\Bigg] + C_F\Bigg[-\frac{205}{128} - \frac{3L_{\tilde{q}}}{16} + \frac{L_{\tilde{q}}^2}{32} + \frac{15\zeta(2)}{16} + \Bigg(-\frac{3}{2} - \frac{L_{\tilde{q}}}{16} + \frac{5\zeta(2)}{4}\Bigg)\frac{m_{\tilde{g}}^2}{m_{\tilde{q}}^2} \\
&+ \Bigg(-\frac{187}{64} - \frac{39L_{\tilde{g}}}{32} - \frac{7L_{\tilde{g}}^2}{8} + \frac{37L_{\tilde{q}}}{32} + \frac{29L_{\tilde{q}}L_{\tilde{g}}}{16} - \frac{15L_{\tilde{q}}^2}{16} + \frac{13\zeta(2)}{8}\Bigg)\frac{m_{\tilde{g}}^4}{m_{\tilde{q}}^4}\Bigg] \\
&+ T_F\Bigg[\frac{28}{9} - \frac{L_t}{12} + \frac{L_t^2}{8} - \frac{5L_{\tilde{q}}}{8} + \frac{3L_{\tilde{q}}^2}{4} - \frac{3\zeta(2)}{4} + \Bigg(\frac{3}{4} - \frac{3L_{\tilde{q}}}{4}\Bigg)\frac{m_{\tilde{g}}^2}{m_{\tilde{q}}^2} + \Bigg(-\frac{1}{2} + \frac{\zeta(2)}{4}\Bigg)\frac{m_t^2}{m_{\tilde{q}}^2} \\
&+ \Bigg(-\frac{13}{16} + \frac{3L_{\tilde{g}}}{8} - \frac{9L_{\tilde{q}}}{8} + \frac{3L_{\tilde{g}}L_{\tilde{q}}}{4} - \frac{3L_{\tilde{q}}^2}{4}\Bigg)\frac{m_{\tilde{g}}^4}{m_{\tilde{q}}^4} + \Bigg(-\frac{5}{2} + \frac{3\zeta(2)}{2}\Bigg)\frac{m_t^2m_{\tilde{g}}^2}{m_{\tilde{q}}^4} \\
&+ \Bigg(\frac{61}{288} - \frac{\zeta(2)}{8} + \frac{L_t}{48} - \frac{L_{\tilde{q}}}{48}\Bigg)\frac{m_t^4}{m_{\tilde{q}}^4}\Bigg] + \frac{X_b}{m_{\tilde{q}}}\Bigg[C_A\Bigg[\Bigg(-\frac{7}{8} + \frac{3L_{\tilde{g}}}{8} - \frac{3L_{\tilde{q}}}{4} - \frac{\zeta(2)}{4}\Bigg)\frac{m_{\tilde{g}}}{m_{\tilde{q}}} \\
&+ \Bigg(-\frac{5}{8} + 2L_{\tilde{g}} - \frac{19L_{\tilde{q}}}{8} + \frac{3L_{\tilde{g}}L_{\tilde{q}}}{8} - \frac{3L_{\tilde{q}}^2}{8} - \frac{\zeta(2)}{4}\Bigg)\frac{m_{\tilde{g}}^3}{m_{\tilde{q}}^3}\Bigg] + C_F\Bigg[\Bigg(-\frac{3}{16} + \frac{3L_{\tilde{q}}}{8} \\
&+ \frac{\zeta(2)}{2}\Bigg)\frac{m_{\tilde{g}}}{m_{\tilde{q}}} + \Bigg(-\frac{13}{16} - \frac{13L_{\tilde{g}}}{16} + \frac{19L_{\tilde{q}}}{16} - \frac{3L_{\tilde{g}}L_{\tilde{q}}}{8} + \frac{3L_{\tilde{q}}^2}{8} + \frac{\zeta(2)}{2}\Bigg)\frac{m_{\tilde{g}}^3}{m_{\tilde{q}}^3}\Bigg] \\
&+ T_F\Bigg[\Bigg(-\frac{3}{4} + \frac{3L_{\tilde{q}}}{2}\Bigg)\frac{m_{\tilde{g}}}{m_{\tilde{q}}} + \Bigg(\frac{7}{4} - \frac{3L_{\tilde{g}}}{4} + \frac{9L_{\tilde{q}}}{4} - \frac{3L_{\tilde{g}}L_{\tilde{q}}}{2} + \frac{3L_{\tilde{q}}^2}{2}\Bigg)\frac{m_{\tilde{g}}^3}{m_{\tilde{q}}^3}
\end{aligned}
$$

$$
\begin{aligned}
&+ \left(\frac{13}{4} - 2\zeta(2)\right)\frac{m_t^2 m_{\tilde{g}}}{m_{\tilde{q}}^3}\Bigg]\Bigg] - \frac{X_t}{m_{\tilde{q}}} T_F \frac{\zeta(2)}{2}\frac{m_t^2 m_{\tilde{g}}}{m_{\tilde{q}}^3} + \frac{X_t X_b}{m_{\tilde{q}}^2} T_F \Bigg[\frac{\zeta(2)}{2}\frac{m_t^2}{m_{\tilde{q}}^2} \\
&+ \left(\frac{3}{4} - 3L_{\tilde{g}} + 3L_{\tilde{q}} + 3\zeta(2)\right)\frac{m_t^2 m_{\tilde{g}}^2}{m_{\tilde{q}}^4} + \left(\frac{5}{9} - \frac{2L_t}{3} + \frac{2L_{\tilde{q}}}{3}\right)\frac{m_t^4}{m_{\tilde{q}}^4}\Bigg] \\
&+ \mathcal{O}\left(\frac{m_{\tilde{g}}^6}{m_{\tilde{q}}^6}, \frac{m_{\tilde{g}}^4 m_t^2}{m_{\tilde{q}}^6}, \frac{m_{\tilde{g}}^2 m_t^4}{m_{\tilde{q}}^6}, \frac{m_t^6}{m_{\tilde{q}}^6}, \frac{X_b m_{\tilde{g}}^5}{m_{\tilde{q}}^6}, \frac{X_t m_{\tilde{g}}^5}{m_{\tilde{q}}^6}\right)\Bigg\}. \qquad (24)
\end{aligned}
$$

We displayed in the previous expressions only the first three terms of the Taylor expansions in the mass ratios. To get an idea about the convergence of the perturbative series we fix the following input parameters: $m_t = 172.4$ GeV, $\alpha_s^{(\mathrm{SQCD})} = 0.120$, $m_{\tilde{q}} = 500$ GeV, $X_q = -4000$ GeV, $X_t = -400$ GeV and let $m_{\tilde{g}}$ vary. Even for $m_{\tilde{g}}/m_{\tilde{q}} = 0.5$, and 2 the approximations given above agree with the exact results with an accuracy better than 1%. For the case of degenerate SUSY masses, *i.e.* $m_{\tilde{g}}/m_{\tilde{q}} = 1$ the accuracy is even below the per-mille level.

5 Numerical results

In this Section we discuss the numerical impact of the two-loop calculations we presented above. A first phenomenological application is the prediction of the strong coupling and the running bottom-quark mass at high-energy scales like $\tilde{M} = 1$ TeV or $\mu_{\mathrm{GUT}} = 10^{16}$ GeV, starting from their low-energy values determined experimentally.

For the energy evolution of the two parameters, we follow the method proposed in Ref. [23]: first, we compute $\alpha_s^{(5)}(\mu_{\mathrm{dec}})$ and $m_b^{(5)}(\mu_{\mathrm{dec}})$ from $\alpha_s^{(5)}(M_Z)$ and $m_b^{(5)}(m_b)$, respectively, using the corresponding i-loop SM RGEs [33]. Here μ_{dec} denotes the energy scale at which the heavy particles are supposed to become active, *i.e.* the scale where the matching between the SM and the MSSM is performed. As pointed out in previous works [34], one can avoid part of the complications related with the occurance of the *evanescent couplings*, performing the change of the regularization scheme from the $\overline{\mathrm{MS}}$ to the $\overline{\mathrm{DR}}$ scheme at the same scale. Nevertheless, one cannot avoid the occurrence of the evanescent coupling α_e in the $\overline{\mathrm{MS}}$-$\overline{\mathrm{DR}}$ relation for the bottom-quark mass. It has to be determined iteratively from the knowledge of the strong coupling at the matching scale. For consistency, the i-loop running parameters have to be folded with $(i-1)$-loop conversion and decoupling relations. Above the decoupling scale, the energy dependence of the running parameters is governed by the i-loop MSSM RGEs [34]. We solved numerically the system of coupled differential equations arising from the two sets of RGEs, and implemented this procedure for $i = 1, 2, 3$.

The decoupling scale is not a physical parameter and cannot be predicted by the theory. It is usually chosen to be of the order of the heavy particle mass in order to circumvent the appearance of large logarithms. At fixed order perturbation theory, it is expected that the relations between the running parameters evaluated at high-energy scales and their low-energy values become less sensitive to the choice of μ_{dec}, once higher order radiative corrections are considered. The dependence on the precise value of the decoupling scale is interpreted as a measure of the unknown higher order corrections. We discuss the scale dependence of $\alpha_s(\mu_{\rm GUT})$ and $m_b(\mu_{\rm GUT})$ in Fig. 2 and Fig. 3, respectively.

For the SM parameters we used $\alpha_s(M_Z) = 0.1189$ [24], where $M_Z = 91.1876$ GeV [50], $m_b(\mu_b) = 4.164$ GeV [25], with $\mu_b = m_b(\mu_b)$, and $M_t = 172.4$ GeV [51]. For the SQCD parameters, we implemented their values for the SPS1a$'$ scenario [11]: $m_{\tilde g} = 607.1$ GeV, $m_{\tilde t_1} = 366.5$ GeV, $m_{\tilde t_2} = 585.5$ GeV, $m_{\tilde b_1} = 506.3$ GeV, $m_{\tilde b_2} = 545.7$ GeV, $A_t^{\overline{\rm DR}}(1~{\rm TeV}) = -565.1$ GeV, $A_b^{\overline{\rm DR}}(1~{\rm TeV}) = -943.4$ GeV, $\mu = 396.0$ GeV, and $\tan\beta = 10.0$.

For the calculation of ζ_{m_b} to two-loop accuracy, the $\overline{\rm DR}$ parameter A_b has to be converted to the renormalization scheme we used here.[1] For the accuracy level we are considering, the one-loop conversion relation is required

$$A_b^{\rm mixed} = A_b^{\overline{\rm DR}} + \Delta A_b\,, \quad \text{where} \quad \Delta A_b = \delta A_b^{\overline{\rm DR}} - \delta A_b^{\rm mixed}\,. \tag{25}$$

The counterterms δA_b^i were defined in Eq. (10) and the superscript i indicates the renormalization scheme. The shift ΔA_b is a finite quantity as it can be explicitly checked. It depends in turn on the running bottom quark mass in the MSSM. We use an iterative method and choose the running bottom quark mass in the SM as the initial parameter. A stable solution is obtained after few iterations. In addition, the energy evolution of the parameter A_b has to be taken into account. We use here the one-loop RGE, that can be derived from Eq. (10).

The dependence on the decoupling scale for $\alpha_s(\mu_{\rm GUT})$ is displayed in Fig. 2. The dotted, dashed and solid lines denote the one-, two-, and three-loop running, where the corresponding exact results for the decoupling coefficients have been implemented. One can see the improved stability of the three-loop results w.r.t. the decoupling-scale variation. The uncertainty induced by the current experimental accuracy on $\alpha_s(M_Z)$, $\delta\alpha_s = 0.001$ [24], is indicated by the hatched band.

In order to get an idea of the effects induced by the SUSY mass parameters on $\alpha_s(\mu_{\rm GUT})$, we show through the dash-dotted line the three-loop results, if the SUSY parameters corresponding to the Snowmass Point SPS2 [53] are adopted. Their explicit values are: $m_{\tilde g} = 784.4$ GeV, $m_{\tilde t_1} = 1003.9$ GeV, $m_{\tilde t_2} = 1307.4$ GeV, $m_{\tilde b_1} = 1296.6$ GeV, $m_{\tilde b_2} = 1520.1$ GeV, and $\tan\beta = 10.0$. The curves induced by the other benchmark points SPSi, with $i = 3, 4, \ldots, 9$ would lie between the two curves displayed here. One clearly notices the great impact of the SUSY-mass pattern on the predicted value of the strong coupling at high energies. Accordingly, for precision studies the explicit mass pattern of heavy particles must be taken into account.

In Fig. 3 the scale dependence for $m_b(\mu_{\rm GUT})$ is shown. The fine-dotted, dashed and solid lines correspond to the exact one-, two-, and three-loop running obtained in the SPS1a$'$ scenario. As explained above, the energy evolution of the running parameters have to be combined with the appropriate matching conditions between the low- and high-energy regimes. More explicitly, in case of m_b we determine its value within SQCD

[1] See Ref. [52] for a detailed discussion.

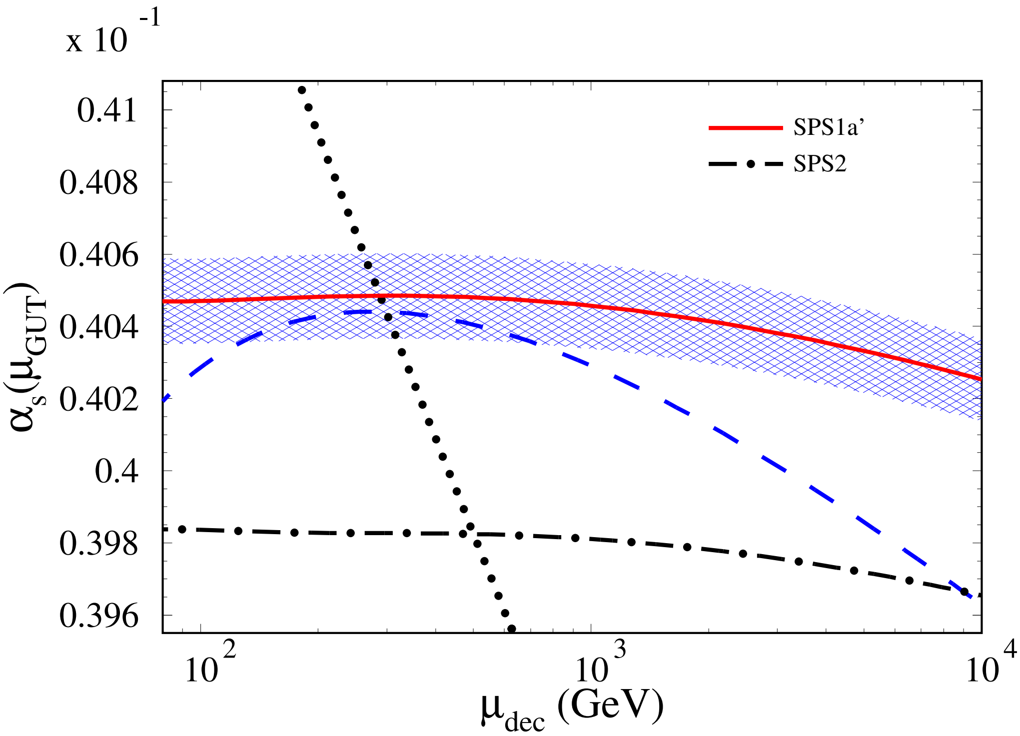

Figure 2: $\alpha_s(\mu_{\rm GUT})$ as a function of $\mu_{\rm dec}$. Dotted, dashed and solid lines denote the one-, two-, and three-loop contributions, respectively, obtained by using for the input parameters their values for the SPS1a$'$ benchmark point. The dash-dotted line shows the three-loop running corresponding to the SPS2 point.

at the energy-scale $\mu_{\rm dec}$ through the relation

$$m_b^{\rm SQCD}(\mu_{\rm dec}) = \frac{m_b^{(5)}(\mu_{\rm dec})}{\zeta_{m_b}(\mu_{\rm dec})}\,, \quad \text{where} \quad \frac{1}{\zeta_{m_b}} = \frac{1}{1+\delta\zeta_{m_b}^{\tan\beta}+\delta\zeta_{m_b}^{\rm rest}}\,. \tag{26}$$

Here $\delta\zeta_{m_b}^{\tan\beta}$ denotes the contributions proportional with $\tan\beta$ and $\delta\zeta_{m_b}^{rest}$ the remaining corrections. For simplicity, we do not show in Eq. (26) the explicit dependence on the MSSM parameters. For the i-loop running analysis, we take into account the $(i-1)$-loop contribution to the Eq. (26). As can be seen from the Figure 3, the three-loop results stabilize the scale dependence and reduce further the theoretical uncertainty.
The dotted line displays the two-loop running bottom-mass, where the contributions proportional with $\tan\beta$ to the one-loop ζ_{m_b} are resummed following the method proposed in Refs. [11, 28]. Within this approach, the matching condition can be written as

$$m_b^{\rm SQCD}(\mu_{\rm dec}) = \frac{m_b^{(5)}(\mu_{\rm dec})}{\zeta_{m_b}^{\rm 1-loop}(\mu_{\rm dec})} \quad \text{and} \quad \frac{1}{\zeta_{m_b}^{\rm 1-loop}} = \frac{1-\delta\zeta_{m_b}^{\rm rest,1-loop}}{1+\delta\zeta_{m_b}^{\tan\beta,\rm 1-loop}}\,. \tag{27}$$

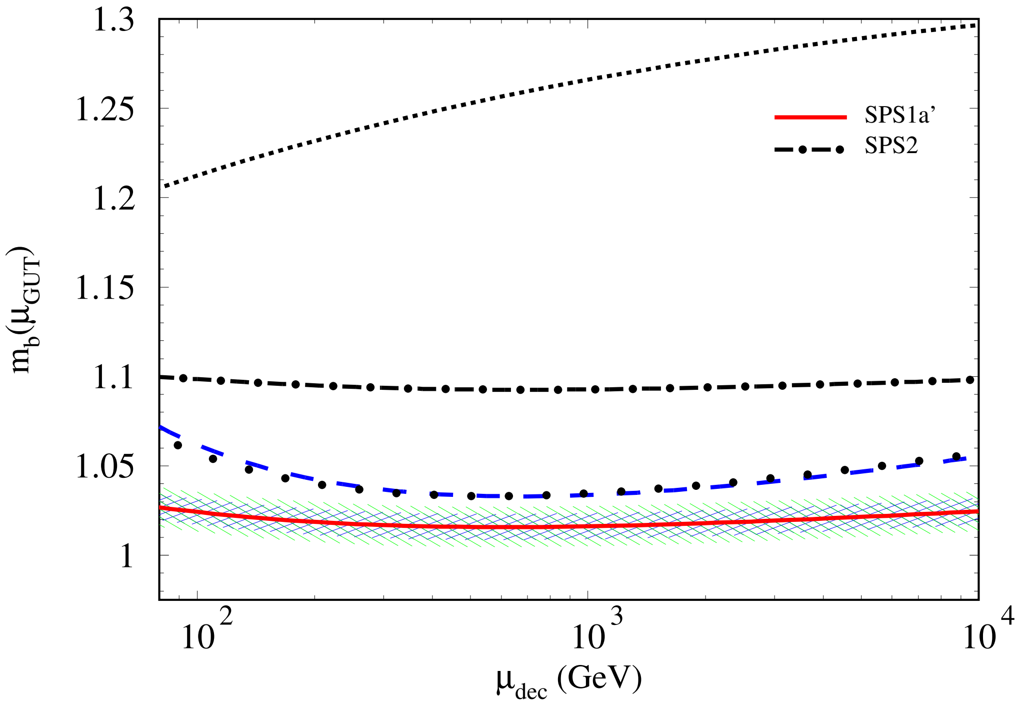

Figure 3: $m_b(\mu_{\rm GUT})$ as a function of $\mu_{\rm dec}$. The fine-dotted, dashed and solid lines denote the one-, two-, and three-loop contributions to the running bottom mass for SPS1a$'$ benchmark point, respectively. The dotted line displays the two-loop running, where the $\tan\beta$ enhanced contributions are resummed according to Ref. [28]. The dash-dotted line represents the three-loop running corresponding to the SPS2 benchmark point.

The superscript $1-$loop indicates the order in perturbation theory at which the individual contributions are evaluated. The authors of Ref. [28] showed that, for a consistent analysis not only the $\tan\beta$-enhanced contributions have to be resummed, but also the next-to-leading logarithms (NLL) $\alpha_s^{i+1}\ln^i(\mu^2/m_b^2)$. In our approach based on i-loop RGEs and $(i-1)$-loop decoupling coefficients the NLL are implicitly resummed. The very good agreement between the two computations can be explained by the fact that at one-loop order $\delta\zeta_{m_b}^{rest}$ is almost an order of magnitude smaller than $\delta\zeta_{m_b}^{\tan\beta}$.
The experimental uncertainty generated by $\delta\,\alpha_s = 0.001$ [24] corresponds to the wider hatched band, and the one due to $\delta\,m_b = 25$ MeV [25] to the narrow band. Let us notice that the three-loop order effects exceed the uncertainty due to current experimental accuracy $\delta\alpha_s$.
Finally, the dash-dotted line shows the three-loop running if the SPS2 scenario is implemented. The differences between the three-loop order results are mainly due to the change of masses of the SUSY particles.

For quantitative comparison, we give in Table 1 the numerical values for $\alpha_s(\mu)$

$\mu = 1000$ GeV					
$\alpha_s(\mu)$	0.0929	$\pm 0.0006\vert_{\delta\,\alpha_s(M_Z)}$		$-0.003\vert_{\mathrm{SPS2}}$	$\pm 0.0001\vert_{\mathrm{th}}$
$m_b(\mu)$	2.164	$\pm 0.017\vert_{\delta\,\alpha_s(M_Z)}$	$\pm 0.015\vert_{\delta\,m_b(m_b)}$	$+0.12\vert_{\mathrm{SPS2}}$	$\pm 0.01\vert_{\mathrm{th}}$

$\mu = \mu_{\mathrm{GUT}}$					
$\alpha_s(\mu)$	0.0405	$\pm 0.0001\vert_{\delta\,\alpha_s(M_Z)}$		$\pm 0.0007\vert_{\mathrm{SPS2}}$	$\pm 0.0001\vert_{\mathrm{th}}$
$m_b(\mu)$	1.016	$\pm 0.011\vert_{\delta\,\alpha_s(M_Z)}$	$\pm 0.007\vert_{\delta\,m_b(m_b)}$	$+0.077\vert_{\mathrm{SPS2}}$	$\pm 0.005\vert_{\mathrm{th}}$

Table 1: Numerical results for the strong coupling and bottom-quark mass for $\mu = 1000$ GeV and $\mu = \mu_{\mathrm{GUT}}$, respectively. The experimental inaccuracy is determined from the to the present uncertainty on $\alpha_s(M_Z)$ and $m_b(m_b)$. The effects of the SUSY-mass parameters are evaluated w.r.t. the SPS2 benchmark point. The theoretical uncertainties due to unknown higher order corrections are estimated from the variation with the decoupling scale for $100\,\mathrm{GeV} \leq \mu_{\mathrm{dec}} \leq 1\,\mathrm{TeV}$.

and $m_b(\mu)$ for $\mu = 1000$ GeV and $\mu = \mu_{\mathrm{GUT}}$, evaluated with three-loop accuracy. For the decoupling scale we choose $\mu_{\mathrm{dec}} = 600$ GeV as at this scale the difference between the two- and three-loop order corrections reaches a minimum. The different sources of uncertainties are explicitly displayed. The theoretical uncertainties due to unknown higher order corrections are estimated from the variation of the three-loop results when the decoupling scale is modified from 100 GeV to 1 TeV. The effects of the SUSY-mass parameters are evaluated as the difference between the three-loop results corresponding to the benchmark points SPS1a′ and SPS2. One can easily see that the impact of the SUSY-mass pattern is at least five times larger than the experimental accuracy.

As already pointed out in the previous sections the unification of the Yukawa couplings is very sensitive to the MSSM parameters. The dependence on the soft SUSY breaking parameters is induced in our approximation only through the decoupling coefficients. They comprise an explicit dependence through the X_b parameter (in the case of ζ_{m_b}) and an implicit one through the squark masses.

The analytical formulae for ζ_s and ζ_m given in Section 4.2 are expressed in terms of the physical squark masses. Since they are not known experimentally, for the following numerical analyses, we computed them making the assumption that the soft SUSY breaking mass parameters defined in the on-shell scheme obey the following relation $M_{\tilde{Q}}(t) = M_{\tilde{D}}(\tilde{M}) = M_{\tilde{U}}(\tilde{M}) = A_f = \pm\mu = \tilde{M}$, where $M_{\tilde{Q}}(t)$ is the on-shell input parameter in the stop-mass matrix.[2] The corresponding input parameter in the sbottom-mass matrix acquires a finite shift of $\mathcal{O}(\alpha_s)$ [54]. Upon diagonalization of the squark-mass matrices Eq. (5), one obtains the on-shell squark masses $m_{\tilde{q}_{1,2}}$. The parameter A_b entering through X_b the one-loop results have to be converted from the on-shell scheme in the renormalization scheme we introduced in Section 2.

[2]See Section 3 for definitions and Refs. [54, 55] for a comprehensive discussion.

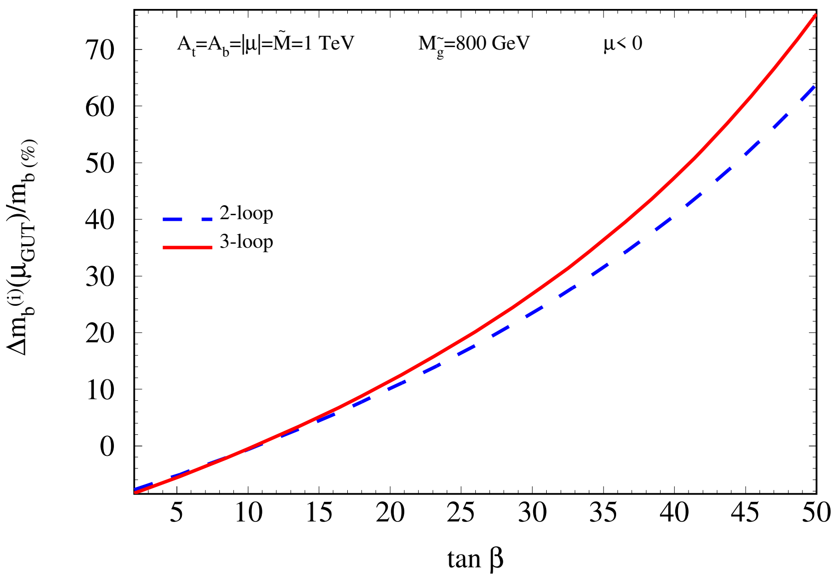

(a)

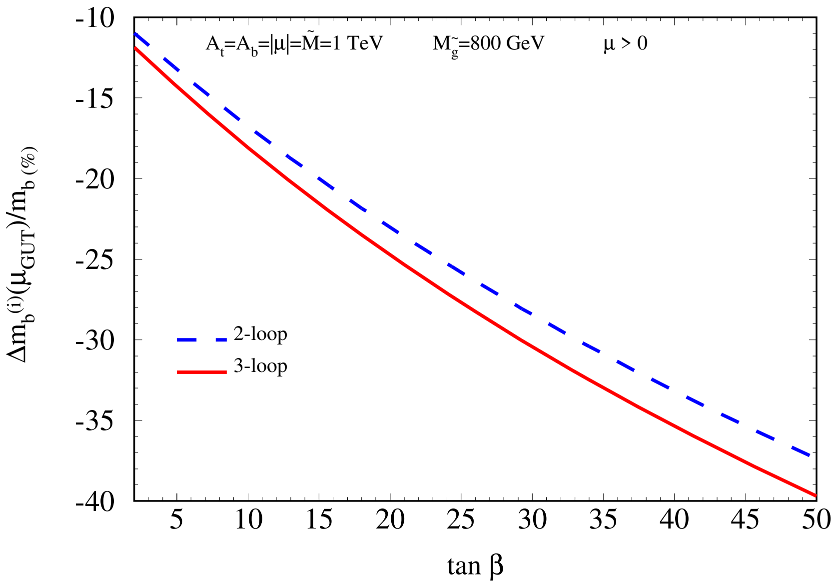

(b)

Figure 4: $\Delta\, m_b/m_b$ as a function of $\tan\beta$ for $\mu < 0$ (a) and $\mu > 0$ (b). The soft SUSY breaking mass parameters are fixed to 1 TeV and the gluino mass to $M_{\tilde{g}} = 800$ GeV.

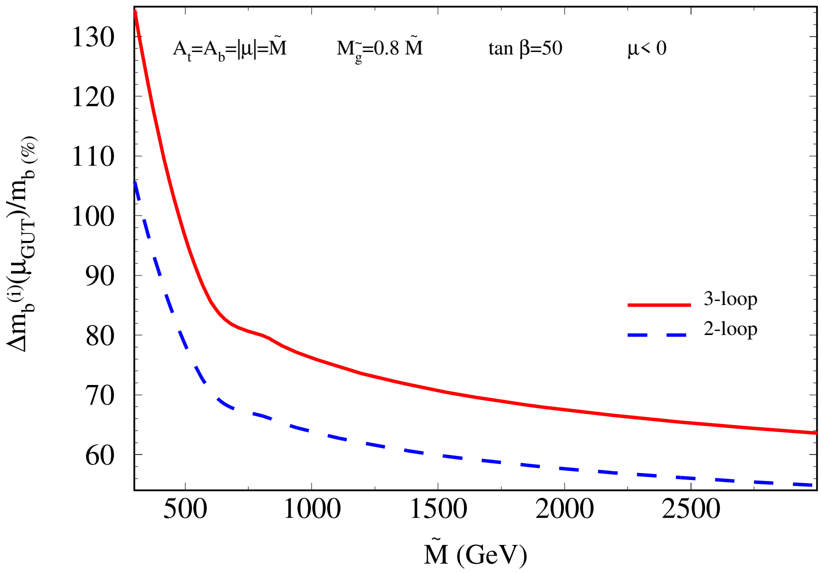

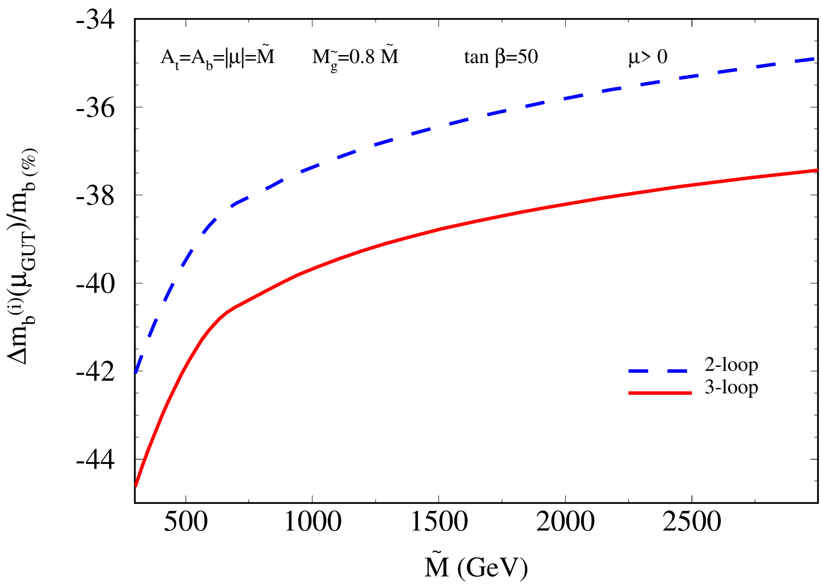

(a)

(b)

Figure 5: $\Delta\, m_b/m_b$ as a function of $\tilde{M}$ for $\mu < 0$ (a) and $\mu > 0$ (b). $\tan\beta$ is fixed to 50 and the gluino mass is $M_{\tilde{g}} = 0.8\tilde{M}$.

In order to estimate the phenomenological impact, we discuss the difference between $m_b(\mu_{\rm GUT})$ evaluated using i-loop running and $(i-1)$-loop decoupling and the one-loop result

$$\frac{\Delta\, m_b^{\rm (i)}}{m_b} = \frac{m_b^{\rm (i\text{-}loop)} - m_b^{\rm (1\text{-}loop)}}{m_b^{\rm (1\text{-}loop)}}\,. \qquad (28)$$

In Fig. 4 we fix the soft SUSY breaking mass parameters to $\tilde{M} = 1$ TeV and $M_{\tilde{g}} = 800$ GeV, and study the dependence of $\Delta\, m_b^{\rm (i)}$ for $i = 2$ (dashed) and $i = 3$ (solid line) as a function of $\tan\beta$. One can clearly see the abrupt increase/decrease of the two- and three-loop order radiative corrections with the increase of $\tan\beta$. Whereas the effects of the the one-loop decoupling can be as large as 65% for $\mu_{\rm SUSY} < 0$ and -37% for $\mu_{\rm SUSY} > 0$, the two-loop corrections are moderate, reaching at most 10% and -3%, respectively.

The numerical effects for large values of $\tan\beta$ are of special interest for the study of Yukawa-coupling unification. In Fig. 5 we show $\Delta\, m_b^{\rm (i)}$ as a function of the soft SUSY breaking mass scale for $\tan\beta = 50$. One can see the increase in size of radiative corrections for lighter SUSY masses. Again, for $\mu_{\rm SUSY} > 0$ the bulk of the corrections are comprised in the two-loop running mass, while the three-loop order effects sum up to few percent. For $\mu_{\rm SUSY} < 0$ and light SUSY masses the three-loop contributions can increase the bottom-quark mass with up to 30%.

6 Conclusions

The knowledge of fundamental parameters at high energies, such as $\tilde{M}$ or $\mu_{\rm GUT}$, are essential for the reconstruction of the theory beyond the SM. In this paper we presented the exact two-loop decoupling coefficients of the strong coupling and the bottom-quark mass within the SQCD. Together with the known three-loop order RGEs they allow predictions of the two parameters at high energies with three-loop accuracy. This level of precision on the theory side is necessary in order to match with the current experimental accuracy. In addition, the dependence on the energy scale at which the supersymmetric particles are integrated out is greatly reduced in this case.

Furthermore, the approach outlined here accounts for the effects induced by the individual mass parameters. They are phenomenologically significant for both parameters and exceed the experimental uncertainty by more than a factor five.

The radiative corrections to the running bottom-quark mass are particularly important for SUSY models with large values of $\tan\beta$. It turns out that for negative values of $\mu_{\rm SUSY}$ the three-loop order contributions can reach up to 30% from the tree-level bottom-quark mass. Furthermore, they clearly stabilize the perturbative behaviour. These features render them indispensable for studies concerning the Yukawa-coupling unification.

Acknowledgements

We would like to thank M. Steinhauser for his continuous support and numerous inspiring discussions and suggestions. We also thank him and R. Harlander for carefully reading the manuscript. L.M. is grateful to K.G. Chetyrkin for enlightening conversations concerning the decoupling approach. This work was supported by the DFG through SFB/TR 9 and by the Graduiertenkolleg “Hochenenergiephysik und Teilchenastrophysik”.

References

[1] S. Dimopoulos, S. Raby and F. Wilczek, Phys. Rev. D **24**, 1681 (1981)

[2] L. E. Ibanez and G. G. Ross, Phys. Lett. B **105**, 439 (1981)

[3] U. Amaldi, W. de Boer and H. Fürstenau, Phys. Lett. B **260** (1991) 447

[4] H. Georgi and S. L. Glashow, Phys. Rev. Lett. **32** (1974) 438.

[5] H. Fritzsch and P. Minkowski, Annals Phys. **93** (1975) 193

[6] L. J. Hall, R. Rattazzi and U. Sarid, Phys. Rev. D **50** (1994) 7048

[7] J. L. Diaz-Cruz, H. Murayama and A. Pierce, Phys. Rev. D **65**, 075011 (2002)

[8] R. Hempfling, Phys. Rev. D **49**, 6168 (1994)

[9] K. Tobe and J. D. Wells, Nucl. Phys. B **663**, 123 (2003)

[10] G. A. Blair, W. Porod and P. M. Zerwas, Eur. Phys. J. C **27** (2003) 263

[11] J. A. Aguilar-Saavedra *et al.*, Eur. Phys. J. C **46** (2006) 43

[12] F. E. Paige, S. D. Protopopescu, H. Baer and X. Tata, [arXiv:hep-ph/0312045]

[13] B. C. Allanach, Comput. Phys. Commun. **143** (2002) 305

[14] W. Porod, Comput. Phys. Commun. **153** (2003) 275

[15] A. Djouadi, J. L. Kneur and G. Moultaka, Comput. Phys. Commun. **176** (2007) 426

[16] S. P. Martin and M. T. Vaughn, Phys. Lett. B **318** (1993) 331

[17] S. P. Martin and M. T. Vaughn, Phys. Rev. D **50** (1994) 2282

[18] I. Jack and D. R. T. Jones, Phys. Lett. B **333** (1994) 372

[19] Y. Yamada, Phys. Rev. D **50** (1994) 3537

[20] D. M. Pierce, J. A. Bagger, K. T. Matchev and R. J. Zhang, Nucl. Phys. B **491** (1997) 3

[21] B. C. Allanach, S. Kraml and W. Porod, JHEP **0303** (2003) 016

[22] R. Harlander, L. Mihaila and M. Steinhauser, Phys. Rev. D **72** (2005) 095009

[23] R. V. Harlander, L. Mihaila and M. Steinhauser, Phys. Rev. D **76** (2007) 055002

[24] S. Bethke, Prog. Part. Nucl. Phys. **58** (2007) 351

[25] J. H. Kühn, M. Steinhauser and C. Sturm, Nucl. Phys. B **778** (2007) 192

[26] D. Noth and M. Spira, arXiv:0808.0087 [hep-ph]

[27] T. Blazek, R. Dermisek and S. Raby, Phys. Rev. D **65**, 115004 (2002)

[28] M. Carena, D. Garcia, U. Nierste and C. E. M. Wagner, Nucl. Phys. B **577** (2000) 88

[29] W. A. Bardeen, A. J. Buras, D. W. Duke and T. Muta, Phys. Rev. D **18** (1978) 3998

[30] W. Siegel, Phys. Lett. B **84** (1979) 193

[31] T. Appelquist and J. Carazzone, Phys. Rev. D **11** (1975) 2856

[32] K. G. Chetyrkin, B. A. Kniehl and M. Steinhauser, Nucl. Phys. B **510** (1998) 61

[33] M. Steinhauser, Phys. Rept. **364** (2002) 247

[34] P. M. Ferreira, I. Jack and D. R. T. Jones, Phys. Lett. B **387** (1996) 80

[35] Y. Schroder and M. Steinhauser, JHEP **0601**, 051 (2006)

[36] K. G. Chetyrkin, J. H. Kuhn and C. Sturm, Nucl. Phys. B **744** (2006) 121

[37] A. V. Bednyakov, Int. J. Mod. Phys. A **22** (2007) 5245

[38] A. Bednyakov, A. Onishchenko, V. Velizhanin and O. Veretin, Eur. Phys. J. C **29** (2003) 87

[39] A. I. Davydychev and J. B. Tausk, Nucl. Phys. B **397**, 123 (1993)

[40] K. G. Chetyrkin and F. V. Tkachov, Nucl. Phys. B **192**, 159 (1981)

[41] P. Nogueira, J. Comput. Phys. **105** (1993) 279

[42] T. Seidensticker, hep-ph/9905298

[43] J. A. M. Vermaseren, arXiv:math-ph/0010025

[44] J. Guasch, J. Sola and W. Hollik, Phys. Lett. B **437** (1998) 88

[45] I. Jack, D. R. T. Jones and K. L. Roberts, Z. Phys. C **62** (1994) 161

[46] I. Jack, D. R. T. Jones, S. P. Martin, M. T. Vaughn and Y. Yamada, Phys. Rev. D **50** (1994) 5481

[47] R. Harlander, P. Kant, L. Mihaila and M. Steinhauser, JHEP **0609** (2006) 053

[48] M. A. Shifman, A. I. Vainshtein and V. I. Zakharov, Phys. Lett. B **78** (1978) 443

[49] J. Guasch, P. Hafliger and M. Spira, Phys. Rev. D **68** (2003) 115001

[50] W. M. Yao *et al.* [Particle Data Group], J. Phys. G **33** (2006) 1

[51] The Tevatron Electroweak Working Group and CDF Collaboration and D0 Collaboration, arXiv:0808.1089 [hep-ex]

[52] S. Heinemeyer, W. Hollik, H. Rzehak and G. Weiglein, Eur. Phys. J. C **39** (2005) 465

[53] N. Ghodbane and H. U. Martyn, in *Proc. of the APS/DPF/DPB Summer Study on the Future of Particle Physics (Snowmass 2001)* ed. N. Graf, arXiv:hep-ph/0201233

[54] A. Bartl, H. Eberl, K. Hidaka, T. Kon, W. Majerotto and Y. Yamada, Phys. Lett. B **402** (1997) 303

[55] A. Djouadi, P. Gambino, S. Heinemeyer, W. Hollik, C. Junger and G. Weiglein, Phys. Rev. D **57**, 4179 (1998)